Utilization the Taguchi Method for Simultaneous Optimization of Microgrid Parameters through the Proposed Criterion for Stability of PLL in Network Connected Converters

Mostafa Ahmadzadeh[1*], Saeedollah Mortazavi[2], Mohsen Saniei[3]
1,2,3- Department of Electrical Engineering, Faculty of Engineering, Shahid Chamran University of Ahvaz, Ahvaz, Iran.
Email: m.ahmadzadeh@mhriau.ac.ir (Corresponding author)
Email: mortazavi_s@scu.ac.ir
Email: m.saniei@scu.ac.ir

Received: August 2017 Revised: November 2017 Accepted: December 2017

ABSTRACT:
Phase-locked loop (PLL) is one of the most important components for the performance, control and grid synchronization of network-connected converters. The stability of PLL are affected by different factors (including the network-side and microgrid-side parameters). Similar to the effect of network-side factors, the effect of microgrid components also play an important role in the stability of PLL. The effect of the microgrid-side parameters on the stability of the PLL has not been studied so far. In this paper, using a new proposed stability criterion and with the aim of stability improvement of PLL, the optimized rate of microgrid-side and network-side Parameters is determined. First, the dynamic model of the mentioned microgrid is simulated in MATLAB software. Then, a Taguchi approach is employed in order to determine the optimal sets of microgrid-side and network-side parameters.

KEYWORDS: Phase-locked Loop Stability, Analytical Modeling, Proposed PLL Stability Criteria, Optimization Microgrid-side Parameters, Taguchi Method, Statistical Methods.

1. INTRODUCTION

Some microgrids are connected to the network via a grid-interface converter. In network-connected applications, PLLs are the most widely used synchronization techniques [1-9]. The phase-locked loop (PLL) is a popular technique for the grid synchronization of network-connected converters. This can be due to the extra benefits of PLL such as simplicity of implementation and its reliability. In all network-connected converters, the synchronization unit is one of the most important parts in the control of network-side converter. In general, we can say that the stability of the PLL can guarantee the network-interface converter.

Dynamic performance and stability of PLL is affected by various factors. In some studies, the impact of network-side factors on the stability of the network-interface converter has been discussed [7, 10]. References [10-11], propose control systems for converters in network- connected applications and show that the performance of such systems can be imperiled by the non-linear performance of PLL.

Also, in [7], [12], issues related to instability of PLL have been investigated. Findings in these papers shows that these unstable conditions are under a weak network (network with large impedance). Reference [18-19], studies PLL instability under island conditions without further discussion. In [7], the dynamics of PLL affected by network impedance changes are described. This article, however, examines the impact of network impedance on small signal stability performance of a three-phase phase-locked loop. In [13-17], small signal stability of network-interface converter is described, but the dynamics of PLL are not discussed. The stability of a network-interface converter and its PLL in network-connected applications are affected by different factors already discussed in various articles. In most of these studies, microgrid side factors (production power fluctuations, energy storage system, loads, etc.) are considered as a constant current or voltage source [14], [20].

This means that the dynamic effect of the microgrid components on the stability of network-interface converter and its' PLL is not considered. Similar to the effect of network side factors on the network-interface converter stability, dynamics of microgrid components also play a role in the stability of the network-interface converter and, in particular, the stability of its' PLL. In this paper, after providing a detailed analytical modeling

of microgrid components, including production power fluctuations, energy storage system, through a proposed criterion for stability of PLL, the optimized rate of microgrid-side and network-side parameters are determined in order to improve the performance of the PLL and consequently the stability of the network-connected converter. First, the model of the mentioned microgrid is simulated in MATLAB software. Then, a Taguchi approach is employed in order to gather simulation results and finally, based on signal-to-noise (S/N) ratio and the analysis of variance (ANOVA), the best sets of microgrid and network parameters that leads to the stability of PLL are determined.

2. MODELING AND CONTROLLING OF STUDIED MICROGRID

For the mentioned study, dynamic modeling is done as a tool for the analysis. For analytic evaluation of the impact of microgrid side factors on stability of PLL, a microgrid composed of distributed generation sources, a hybrid storage system (batteries and super-capacitors) with a grid -interface bi-directional converter, DC and AC loads, and an energy management system are considered. Fig. 1, shows a schematic of the microgrid along with the grid-interface converter. In this figure, the inverter is connected to the DC bus. The DC bus is equal to a capacitor with capacitance C_{eq}.

According to (1), the small-signal model of system represents the amount of fluctuations of average variables around the operating point. In this Equation, the order of $\boldsymbol{X}, \widetilde{\boldsymbol{x}}, \overline{\boldsymbol{x}}$ is the amount of average variable at the operating point, the small signal term of average variable, and the average variable, respectively [15].

$$\bar{x} = X + \tilde{x} \tag{1}$$

If we extend (1) to all of the state Equations corresponding to microgrid's components and assume that the small signal term of the average variables and the changes of average variables (derivatives) at the operating point are insignificant, the network operating point will be achieved by solving the Equations. Due to nonlinearity of the average model, the obtained average model equations should be linearized around the operating point. The above linearization process will result in state (2):

$$\frac{d\tilde{x}(t)}{dt} = A\tilde{x}(t) + B\tilde{u}(t) \tag{2a}$$

$$\tilde{y}(t) = C\tilde{x}(t) + D\tilde{u}(t)$$

$$\tilde{x}(t) = [\tilde{\imath}_{b,}\tilde{\imath}_{sc}, \tilde{u}_{dc}, \tilde{\imath}_{l1d}, \tilde{\imath}_{l1q}, \tilde{\imath}_{l2d}, \tilde{\imath}_{l2q}, \tilde{\imath}_{LLd}, \tilde{\imath}_{LLq}, \tilde{u}_{cfild}, \tilde{u}_{cfilq}, \tilde{u}_{sc,}\tilde{u}_{pd,}\tilde{u}_{pq}, \tilde{C}, \tilde{\theta}_P] \tag{2a}$$

$$\tilde{y}(t) = [\tilde{\imath}_{b,}\tilde{\imath}_{sc}, \tilde{u}_{dc}, \tilde{\imath}_{l1d}, \tilde{\imath}_{l1q}, \tilde{\imath}_{l2d}, \tilde{\imath}_{l2q}, \tilde{u}_{sc,}\tilde{u}_{pd,}\tilde{u}_{pq}\ \tilde{C}, \tilde{\theta}_P] \tag{2c}$$

$$\tilde{u}(t) = \left[\tilde{d}_1, \tilde{d}_2, \tilde{d}_d\ , \tilde{d}_q, \tilde{u}_{netd}, \tilde{u}_{netq}, i_{Gl}\right] \tag{2d}$$

In the above Equation, $\tilde{x}(t)$ ،$\tilde{y}(t)$ ،$\tilde{u}$ are the network state variable, the output vector, and the input vector, respectively. Since (2) has been linearized, we can achieve its Laplace transform, which will be the following equation:

$$sX(s) = AX(s) + BU(s) \tag{3a}$$

$$Y(s) = CX(s) + DU(s) \tag{3b}$$

The relationship between the input and output variables (Laplace transform function) is in (4):

$$Y(s) = [C(sI - A)^{-1}B + D]U(s) = G_H U(s) \tag{4}$$

Matrices A, B, C, and D are in the (5a-5d).

Where:

C_{sc}، R_s ، u_{sc}، u_b، i_{sc}، i_b، L_{22}، L_{11}، d_2، d_1، R_{L2} ، R_{L1}، i_{l1d}، $i_{l1q}, d_d, d_q, i_{Gl\ ,}u_{dc},, Z_L, Z_{net}$,

are the equivalent capacity of super-capacitor, the equivalent series resistance of super-capacitor, the super-capacitor voltage, the battery voltage, the super-capacitor current, the battery current, the inductance of output filter of super-capacitor converter, the inductance of output filter of battery converter, the duty cycle of super-capacitor converter, the duty cycle of battery converter, the equivalent resistance of power losses related to the switches of super-capacitor converter, and the equivalent resistance of power losses related to the switches of battery converter, d-component instantaneous current of grid-interface converter, the q-component instantaneous current of grid-interface converter, the d-component duty cycle of grid-interface converter, the q-component duty cycle of grid- interface converter, differences between the current of consumable load and the current produced by distributed generation sources, the instantaneous voltage of DC bus, the local load(ohmic load(R_L) parallel with inductive load(L_L)) impedance and the network impedance respectively.

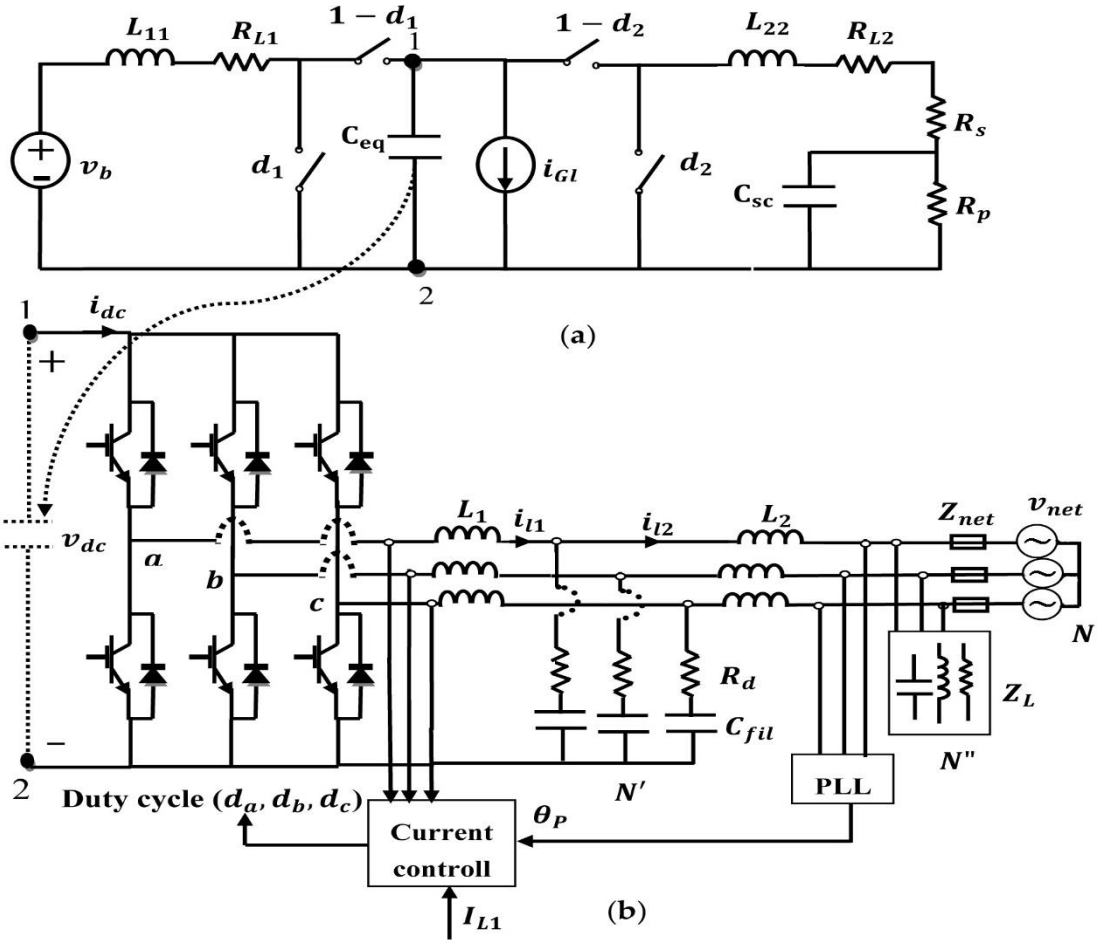

Fig. 1. Schematic of the micro-grid along with the network-interface converter.

$$A=\begin{bmatrix}
K_{b44} & 0 & K_{b22} & 0 & 0 & 0 & 0 & 0 & 0 & 0 & 0 & K'_{1sc} & 0 & 0 & 0 & 0\\
0 & K'_{4sc} & K'_{2sc} & 0 & 0 & 0 & 0 & 0 & 0 & 0 & 0 & K'_{1sc} & 0 & 0 & 0 & 0\\
K_{11dc} & K_{33dc} & 0 & -\frac{D_d}{C_{eq}} & -\frac{D_q}{C_{eq}} & 0 & 0 & 0 & 0 & 0 & 0 & 0 & 0 & 0 & 0 & 0\\
0 & 0 & \frac{D_d}{L_1} & -\frac{R_d}{L_1} & \omega_p & \frac{R_d}{L_1} & 0 & 0 & 0 & -\frac{1}{L_1} & 0 & 0 & 0 & 0 & 0 & 0\\
0 & 0 & \frac{D_q}{L_1} & -\omega_p & -\frac{R_d}{L_1} & 0 & \frac{R_d}{L_1} & 0 & 0 & 0 & -\frac{1}{L_1} & 0 & 0 & 0 & 0 & 0\\
0 & 0 & 0 & K_{11} & 0 & -K_{22} & \omega_p & -K_{44} & 0 & K_{33} & 0 & 0 & 0 & 0 & 0 & 0\\
0 & 0 & 0 & 0 & K_{11} & -\omega_p & -K_{22} & 0 & -K_{44} & 0 & K_{33} & 0 & 0 & 0 & 0 & 0\\
0 & 0 & 0 & K'_{33} & 0 & K'_{22} & 0 & K'_{11} & \omega_p & K'_{44} & 0 & 0 & 0 & 0 & 0 & 0\\
0 & 0 & 0 & 0 & K'_{33} & 0 & K'_{22} & -\omega_p & K'_{11} & 0 & K'_{44} & 0 & 0 & 0 & 0 & 0\\
0 & 0 & 0 & \frac{1}{C_{fil}} & 0 & -\frac{1}{C_{fil}} & 0 & 0 & 0 & 0 & \omega_p & 0 & 0 & 0 & 0 & 0\\
0 & 0 & 0 & 0 & \frac{1}{C_{fil}} & 0 & -\frac{1}{C_{fil}} & 0 & 0 & -\omega_p & 0 & 0 & 0 & 0 & 0 & 0\\
0 & -K_{4sc} & K_{2sc} & 0 & 0 & 0 & 0 & 0 & 0 & 0 & 0 & K_{1sc} & 0 & 0 & 0 & 0\\
0 & 0 & 0 & K''_1 & 0 & K''_7 & K''_8 & K''_2 & K''_3 & K''_3 & 0 & 0 & 0 & 0 & 0 & 0\\
0 & 0 & 0 & 0 & K''_1 & K''_9 & K''_{10} & K''_4 & K''_5 & 0 & K''_6 & 0 & 0 & 0 & 0 & 0\\
0 & 0 & 0 & 0 & 0 & 0 & 0 & 0 & 0 & 0 & 0 & 0 & 0 & -K_{iPLL} & 0 & 0\\
0 & 0 & 0 & 0 & 0 & 0 & 0 & 0 & 0 & 0 & 0 & 0 & 0 & -K_{pPLL} & 1 & 0
\end{bmatrix} \quad (5a)$$

$$B=\begin{bmatrix} K_{b33} & 0 & 0 & 0 & 0 & 0 & 0 \\ 0 & K'_{3sc} & 0 & 0 & 0 & 0 & 0 \\ K_{22dc} & K_{44dc} & -\frac{I_{lid}}{C_{eq}} & -\frac{I_{liq}}{C_{eq}} & 0 & 0 & K_{55dc} \\ 0 & 0 & \frac{U_{DC}}{L_1} & 0 & 0 & 0 & 0 \\ 0 & 0 & 0 & \frac{U_{DC}}{L_1} & 0 & 0 & 0 \\ 0 & 0 & 0 & 0 & K_{55} & 0 & 0 \\ 0 & 0 & 0 & 0 & 0 & K_{55} & 0 \\ 0 & 0 & 0 & 0 & K'_{55} & 0 & 0 \\ 0 & 0 & 0 & 0 & 0 & K'_{55} & 0 \\ 0 & 0 & 0 & 0 & 0 & 0 & 0 \\ 0 & 0 & 0 & 0 & 0 & 0 & 0 \\ 0 & -K_{3sc} & 0 & 0 & 0 & 0 & 0 \\ 0 & 0 & 0 & 0 & K''_{11} & 0 & 0 \\ 0 & 0 & 0 & 0 & 0 & K''_{12} & 0 \\ 0 & 0 & 0 & 0 & 0 & 0 & 0 \\ 0 & 0 & 0 & 0 & 0 & 0 & 0 \end{bmatrix} \quad (5b)$$

$$C = I \quad (5c)$$

$$D = 0 \quad (5d)$$

3. THE CONTROLLER OF MICROGRID AND GRID- SIDE CONVERTER

As shown in Fig. 2, the proposed control system is a complex system and its aim is to maintain the DC bus voltage $\boldsymbol{u_{dc}}$ by regulating the battery, the super-capacitor and the grid-interface converter currents. Thus, the instantaneous voltage $\boldsymbol{u_{dc}}$ is first compared with its reference value. Its error passes from PI controller, and the share of the battery, the super-capacitor and the grid-interface converter compensation are also determined. To specify the contribution of each of these elements to the compensation, various indicators can be taken into account. In this article, toward increasing the battery life, and also because the super-capacitor has a high response speed, sudden changes in power are compensated by a super-capacitor. This means that the high frequency error terms will be compensated by the super-capacitor, lower frequency terms by the battery and the rest will be compensated by means of the grid-interface converter.

The mentioned frequency bandwidth is determined by a low-pass filter for battery, a band-pass filter for grid-interface converter and the rest for the grid-interface converter. In this control system, $\boldsymbol{\tau_1}$ ،$\boldsymbol{\tau_2}$ ،$\boldsymbol{I^*_b}$ ، $\boldsymbol{I^*_{SC}}$ ،$\boldsymbol{I^*_{l1d}}$ ،$\boldsymbol{I^*_{l1q}}$،$\boldsymbol{i_{dis}}$ ،$\boldsymbol{u^*_{dc}}$ are the time constant of low-pass filter, the time constant of band-pass filter, the reference charging or discharging current of battery, the reference charging or discharging current of super-capacitor, the d-component reference current of grid-interface converter, the q-component reference current of grid-interface converter, the error current caused by the difference between the instantaneous and reference voltage of DC bus and the reference voltage of DC bus, respectively.

4. PROPOSED CRITERION FOR THE STABILITY OF SRF-PLL

Almost all PLLs are comprised of three basic parts: phase detector (PD), loop filter (LF), and voltage controlled oscillator (VCO) [3]. Fig. 3, shows the overall structure of a conventional SRF-PLL. The phase angle of input signal is compared with the feedback of the output of oscillator, and the error signal is produced proportional to the difference between the input and output phase angles. Phase detector output consists of harmonic components that are passed by the low-pass filter. Controlled output voltage of the loop filter (which is a function of frequency) enters into the oscillator and produces a phase output. The output signal (which is in the form of phase angle) goes back to the phase detector with a negative feedback. The output signal of oscillator is compared with the input; if their frequency were different, the output frequency of oscillator is changed to be equal with the input frequency. In this PLL, as can be seen in Fig. 4, a three-phase input voltage ($\tilde{u}_{pabc}$) is transformed into the rotating frame (u_{pd} ,u_{pq}) using Clarke and Park transformation.

Using a feedback loop, the angular position of dq framework is controlled in a way that one of the d or q voltage components is zero. If we assume that the network voltage $\tilde{u}_{net}(\theta_{net})$, is a vector that is spinning with a synchronous angle θ_{net}, the angle θ_P would be coincident on the angle θ_{net} to make the output current of inverter synchronized with the network voltage.

According to the Park transformation matrix, we will have:

$$\begin{bmatrix} u_{pd} \\ u_{pq} \\ u_{p0} \end{bmatrix} =$$

$$\frac{2}{3}\begin{bmatrix} \cos(\theta_P) & \cos(\theta_P - \frac{2\pi}{3}) & \cos(\theta_P + \frac{4\pi}{3}) \\ \sin(\theta_P) & \sin(\theta_P - \frac{2\pi}{3}) & \sin(\theta_P + \frac{4\pi}{3}) \\ \frac{1}{2} & \frac{1}{2} & \frac{1}{2} \end{bmatrix} \times$$

$$\begin{bmatrix} u_{net}\cos(\theta_{net}) \\ u_{net}\cos(\theta_{net} - \frac{2\pi}{3}) \\ u_{net}\cos(\theta_{net} + \frac{2\pi}{3}) \end{bmatrix} \quad (6a)$$

$$u_{pq} = u_{net}\sin(\theta_{net} - \theta_P) \quad (6b)$$

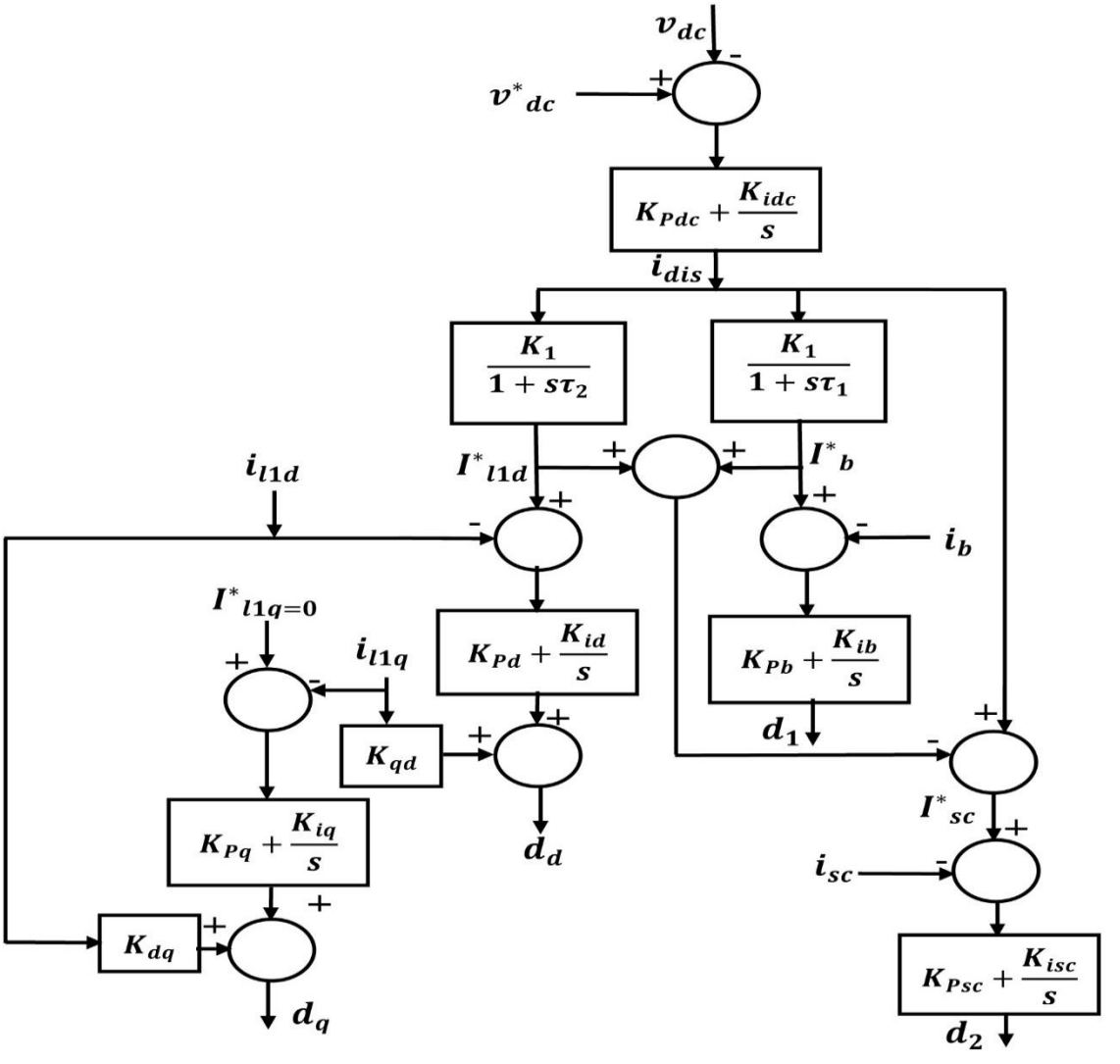

Fig. 2. The proposed control system.

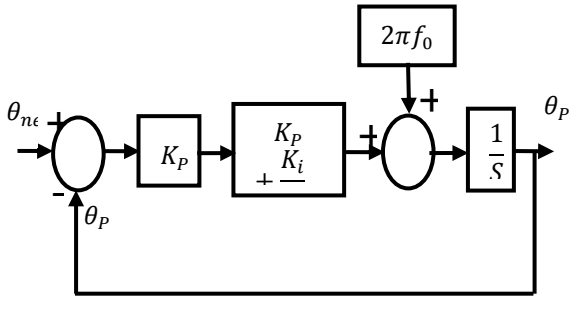

Fig. 3. Linear model of SRF-PLL [15].

According to (6b), if we want to match angle θ_P on the angle θ_{net}, then up_q must be equal to zero. It should be noted that this compliance, in addition to maintaining synchronization between the output voltage of microgrid and the voltage of main network will also contribute to the stability of PLL. (Because up_q enters

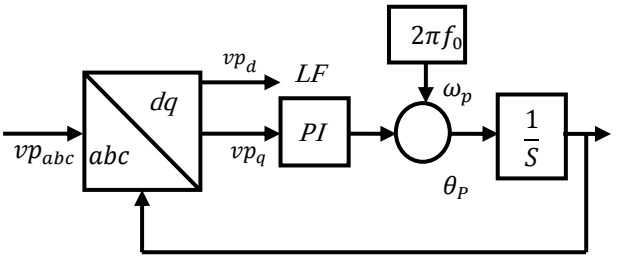

Fig. 4. SRF-PLL [1, 11].

Into the integrator, its non- zero value can lead to instability of PLL. Therefore, the condition $up_q = 0$ is considered to be as a proposed criterion for the stability of the PLL. According to (4), the output current of

inverter $\tilde{\imath}_{l2}(\theta_P)$ has two components $\tilde{\imath}_{l2q}$ and $\tilde{\imath}_{l2d}$ that can be obtained as follows:

$$\tilde{\imath}_{l2d} = G_{61}.\tilde{d}_1 + G_{62}.\tilde{d}_2 + G_{63}.\tilde{d}_d + G_{64}.\tilde{d}_q - Y_{65}.\tilde{u}_{netd} + G_{66}.\tilde{u}_{netq} + G_{67}.\tilde{\imath}_{Gl} \quad (7)$$

$$\tilde{\imath}_{l2q} = G_{71}.\tilde{d}_1 + G_{72}.\tilde{d}_2 + G_{73}.\tilde{d}_d + G_{74}.\tilde{d}_q - Y_{75}.\tilde{u}_{netd} + G_{76}.\tilde{u}_{netq} + G_{77}.\tilde{\imath}_{Gl} \quad (8)$$

According to the above relations, and considering that output current of inverter is a vector, this current can be shown as follows:

$$\tilde{\imath}_{l2}(\theta_P) = I_{l2}e^{j\theta_P} \quad (9a)$$

$$I_{l2} = \sqrt{(|\tilde{\imath}_{l2d}|^2 + |\tilde{\imath}_{l2q}|^2)} \quad (9b)$$

In $(9a)$, I_{l2} and θ_P are the amplitude and the angle of output current of inverter, respectively. This angle was determined by the PLL. In Fig. 5, it is assumed that the PLL position is after the inverter LCL filter. In this case, the voltage which the PLL measures ($\tilde{u}_{pabc}$) is affected by two factors: the network-side parameters and the microgrid-side parameters. Also, it is assumed that Z_{net} and $\tilde{u}_{net}(\theta_{net})$ are the impedance and the voltage of the network, respectively. Therefore, the input voltage to the PLL will be as follows:

$$\tilde{u}_{pabc} = \tilde{u}_{mgrid} + \tilde{u}_{net} \quad (10)$$

In this regard, $\tilde{u}_{net}$ and $\tilde{u}_{mgrid}$ are the voltage caused by network -side factors connected to the Microgrid (the main grid) and the voltage caused by microgrid- side factors, respectively. In next section, the effect of network -side and grid-side factors on condition $up_q = 0$ and as a result proposed criterion for the stability of the PLL is investigated.

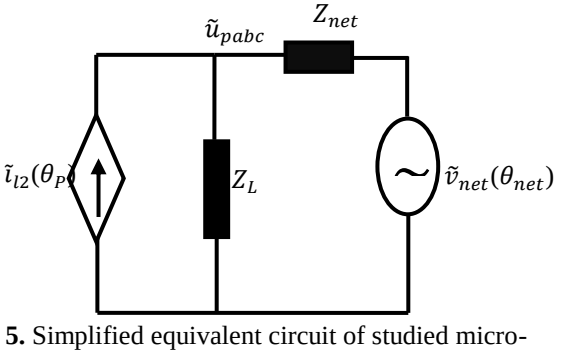

Fig. 5. Simplified equivalent circuit of studied micro-grid and grid-side converter.

5. DETERMINING THE OPTIMAL MICROGRID-SIDE PARAMETERS

The Optimization Process is one of the most important activities in today's competitive industry. The high cost of research and development projects has necessitated the exploitation of methods of experiment design which can determine the impressive factors on processes with the least number of testing. Methods of experiment design have widely been used in the past two decades to achieve this goal. Compared with other commonly-used methods such as full factorial design, fractional factorial, Latin Squares, etc., Taguchi experimental design method, in addition to having this role, has found much wider applicability because of being more comprehensive in some parts of the industry.

Taguchi method can be considered as a statistical method to optimize and improve the quality of each process. In some cases, the traditional experimental designs are very complicated and sometimes infeasible. When the number of parameters in a process is large, a great number of experiments (simulations) is required to optimize the parameters of the experimental design method. Taguchi method uses a specific orthogonal array to resolve this problem, and investigate all parameters by using a few tests (simulations).

Taguchi method is widely used in engineering analysis with the aim of obtaining information about the behavior of a process. The biggest advantages of this method include saving the number of experiments (simulations), saving the time, reducing the costs, etc.

5.1. Testing and Analysis

The purpose of the study was to evaluate the effects of the micro-grid and network parameters on the stability of PLL. The study simultaneously aimed at determining the optimal values of these parameters to improve the stability of PLL and thereby improve the stability of the network-side converter.

For this purpose, C_{eq} , L_{11}, C_{sc}, L_{22}, ‘i_{Gl}‘τ‘L_2‘L_1‘C_f‘R_L‘L_L, z_{net} are considered as microgrid electrical parameters and z_{net} as the main network parameter. In contrast, $up_q = 0$ is determined as proposed PLL stability criterion and it is considered as the most important characteristic of the output process. Each regulatory parameter (microgrid and network-side parameters) has been evaluated in three levels. Table 1 shows the regulatory parameters of the process along with their levels.

To achieve the aims of this study, a set of simulations data related to the process is required. According to the number of parameters and their levels, the total number of states (tests or simulations) is obtained from $n = L^K$. In this equation, n is the number of experiments, L is the number of levels, and K is the number of considered parameters. In this study, there

are 12 parameters in each of the 3 levels. Therefore, the total number of simulations will be equal to 531,441 Tests (simulations). It is clear that carrying out this large number of tests is very time consuming. Moreover, it is not cost-effective. Therefore, Taguchi experimental design approach is used to collect the required data. Taguchi provides a practical approach regarding the quality control of manufacturing industries.

Table 1. Different levels of process variables.

Parameter	Level 1	Level 1	Level 1
L_{11}	0.1 mH	1 mH	10 mH
L_{22}	0.1 mH	1 mH	10 mH
C_{sc}	0.1 F	1 F	5 F
C_{eq}	0.1 mF	1 mF	100mF
L_1	0.5 mH	5 mH	10 mH
τ	0.50 s	5 s	10 s
R_L	0.5 Ω	2 Ω	3 Ω
L_2	0.5 mH	5 mH	10 mH
C_{fil}	0.1 mF	5 mF	10 mF
Z_{net}	10 Ω	40 Ω	90 Ω
L_L	50 mH	100 mH	200 mH

The main objectives of Taguchi method include determining the effect of each parameter on the output process and determining the optimal levels of these parameters. Taguchi method achieves these goals by analyzing simulations data which have been collected in predetermined terms. In this study, experiments have been designed by Minitan17 software. Taguchi suggests an $\mathbf{L_{27}}$ orthogonal array for 12 input factors and 3 levels. Resultantly, 27 tests (simulations) were performed according to the levels shown in Table 2, and the amount of u_{Pq} was measured through the simulation of the mentioned microgrid (Fig. 1) in MATLAB software. The measured value of u_{Pq} is provided in column 14 in Table 2.

5.2. Analyzing the Signal to Noise Ratio

Signal to noise ratio, represents the sensitivity of the studied characteristic to Input factors in a controlled process [16]. The optimum condition is detected by determining the effect of each input factor on output characteristic. From the perspective of the characteristic of the output process, it can be divided into three categories: the less, the better (smaller is better), the closer to nominal amount, the better (nominal is best), and the bigger, the better (larger is better). Taguchi has offered different equations to calculate the signal to noise ratio in terms of the relevance of the desired characteristic to any of the three mentioned groups. In general, the highest ratio (S/N) is always desirable in each test. The output measured in this study is u_{Pq}which is placed in the category the smaller is better. Therefore, the following equation is used to calculate the signal to noise ratio.

$$\frac{\mathrm{S}}{\mathrm{N}} = -10\log_{10}\left(\frac{1}{\mathrm{n}}\sum_{\mathrm{i}=1}^{\mathrm{n}}(\mathrm{y_i})^2\right) \quad (11)$$

In the above equation, *n* is the frequency of each test, and y_i is *i*-th measured output. Signal to noise ratio is calculated for each of the 27 experiments performed using the equation mentioned above and is shown in the last column in Table 2. In this study, each of the tests was done only once and thus, *n* is equal to one.

5.3. Analysis of Variance

Because in the Taguchi experiments, only some parts of the possible cases are tested, to ensure the accuracy of the final results, appropriate statistical methods should be used. Analysis of variance is a statistical method that calculates the degree of confidence and determines the contribution percentage of each variable on the output process. Then, the statistical analyses conducted on the results of the experiment (simulations) in micro-grid for the PLL stability are provided. Table 3, shows the analysis of variance for q-axis component of the voltage measured by the PLL (u_{Pq}). This analysis has been carried out based on a confidence level of 95% (uncertainty 5%). Columns 2-7 in the Table 3 show the degrees of freedom (DF) for each parameter, the sum of squares (seqSS), the adjusted sum of squares (Adj SS), the average sum of squares (Adj MS), F statistic, P statistic, and the effect of each input parameter on the desired output (P%), respectively. P statistics is used to determine the significant influence of each parameter on the output. According to the analysis which was based on 95% confidence level, if P value for each parameter is less than 0.05, it will be indicative of the significant influence of each parameter on the output. As is shown in the Table 3, P value is less than 0.05 for some parameters.

Table 3 shows the effect of each micro-grid and main grid parameter on the q-axis component of the voltage measured by the PLL (u_{Pq}) and thus the stability of PLL. It is clear that the inductive local load (with inductanceL_L) has the greatest impact on the stability of PLL by more than 14 percent. Other parameters are in order of importance $\tau, R_L,$ i_{Gl} , $\mathrm{L}_2, z_{net}, C_f$, $\mathrm{L}_1, \mathrm{L}_{11}, C_{eq}, \mathrm{C}_{\mathrm{sc}}$،$\mathrm{L}_{22}$. In the present study, the amount of signal to noise (S / N) was calculated for the results of all the tests using (11).

Then, the mean value of the signal to noise ratio was obtained for each level of each parameter tested. Fig. 6, shows the mean signal to noise ratio for each of the 12 adjustment parameters in the u_{Pq}. As mentioned earlier, high levels of signal to noise ratio are always desirable. Therefore, based on the mean signal to noise ratio of each adjustment parameter, it is possible to determine their optimal levels. According to Fig. 6, the best levels for the parameters of the micro-grid and network to achieve the best stability of the grid-side converter and the PLL stability are in table 4.

Table 2. Output results of simulation for measurement of v_{pq}.

Simulation Number	L_1	L_2	L_{11}	L_{22}	C_{eq}	C_{fil}	R_{LL}	L_{LL}	C_{sc}	R_g	τ	i_{Gl}	v_{pq}	S/N
1	1	1	1	1	1	1	1	1	1	1	1	1	0.0714	18.5776
2	1	1	1	1	2	2	2	2	2	2	2	2	0.2857	09.8591
3	1	1	1	1	3	3	3	3	3	3	3	3	0.5000	06.0206
4	1	2	2	2	1	1	1	2	2	2	3	3	0.1176	17.1272
5	1	2	2	2	2	2	2	3	3	3	1	1	0.3319	08.9442
6	1	2	2	2	3	3	3	1	1	1	2	2	0.2184	12.2950
7	1	3	3	3	1	1	1	3	3	3	2	2	0.1638	14.7938
8	1	3	3	3	2	2	2	1	1	1	3	3	0.0504	20.0000
9	1	3	3	3	3	3	3	2	2	2	1	1	0.2647	10.8818
10	2	1	2	3	1	2	3	1	2	3	1	2	0.3025	09.0329
11	2	1	2	3	2	3	1	2	3	1	2	3	0.2268	12.0412
12	2	1	2	3	3	1	2	3	1	2	3	1	0.1260	15.7031
13	2	2	3	1	1	2	3	2	3	1	3	1	0.0840	18.3156
14	2	2	3	1	2	3	1	3	1	2	1	2	0.2731	10.2544
15	2	2	3	1	3	1	2	1	2	3	2	3	0.1848	13.9795
16	2	3	1	2	1	2	3	3	1	2	2	3	0.2815	09.8699
17	2	3	1	2	2	3	1	1	2	3	3	1	0.0294	22.1026
18	2	3	1	2	3	1	2	2	3	1	1	2	0.1176	16.9054
19	3	1	3	2	1	3	2	1	3	2	1	3	0.2689	10.4574
20	3	1	3	2	2	1	3	2	1	3	2	1	0.1680	14.0500
21	3	1	3	2	3	2	1	3	2	1	3	2	0.0924	18.0618
22	3	2	1	3	1	3	2	2	1	3	3	2	0.1638	14.1372
23	3	2	1	3	2	1	3	3	2	1	1	3	0.2521	11.2133
24	3	2	1	3	3	2	1	1	3	2	2	1	0.0040	49.1186
25	3	3	2	1	1	3	2	3	2	1	2	1	0.0966	17.8219
26	3	3	2	1	2	1	3	1	3	2	3	2	0.0084	30.9031
27	3	3	2	1	3	2	1	2	1	3	1	3	0.1974	13.0964

Table 3. Result of analysis of variance of signal to noise ratio.

Parameter	DF	Adj SS	Adj MS	F value	P value	$P(\%)$
L_1	2	0.03144	0.015721	4.32	0.039	8.05
L_2	2	0.03845	0.019224	5.28	0.023	10.25
R_L	2	0.04537	0.022686	6.23	0.014	12.04
L_L	2	0.05327	0.026634	7.32	0.008	14.03
R_g	2	0.03845	0.019224	5.28	0.023	10.25
τ	2	0.04576	0.022882	6.29	0.013	12.16
i_{Gl}	2	0.04535	0.022675	6.23	0.014	12.04
C_{fil}	2	0.03846	0.019229	4.56	0.034	9.03
L_{11}	2	0.001634	0.000817	2.40	0.294	4.35
C_{eq}	2	0.000670	0.000335	0.98	0.504	1.84
L_{22}	2	0.000493	0.000246	0.72	0.58	1.32
C_{sc}	2	0.000591	0.000301	0.87	0.510	1.52
$Error$	2	0.03667	0.003056	-	-	3.12
Total	26	0.376196	-	-	-	100

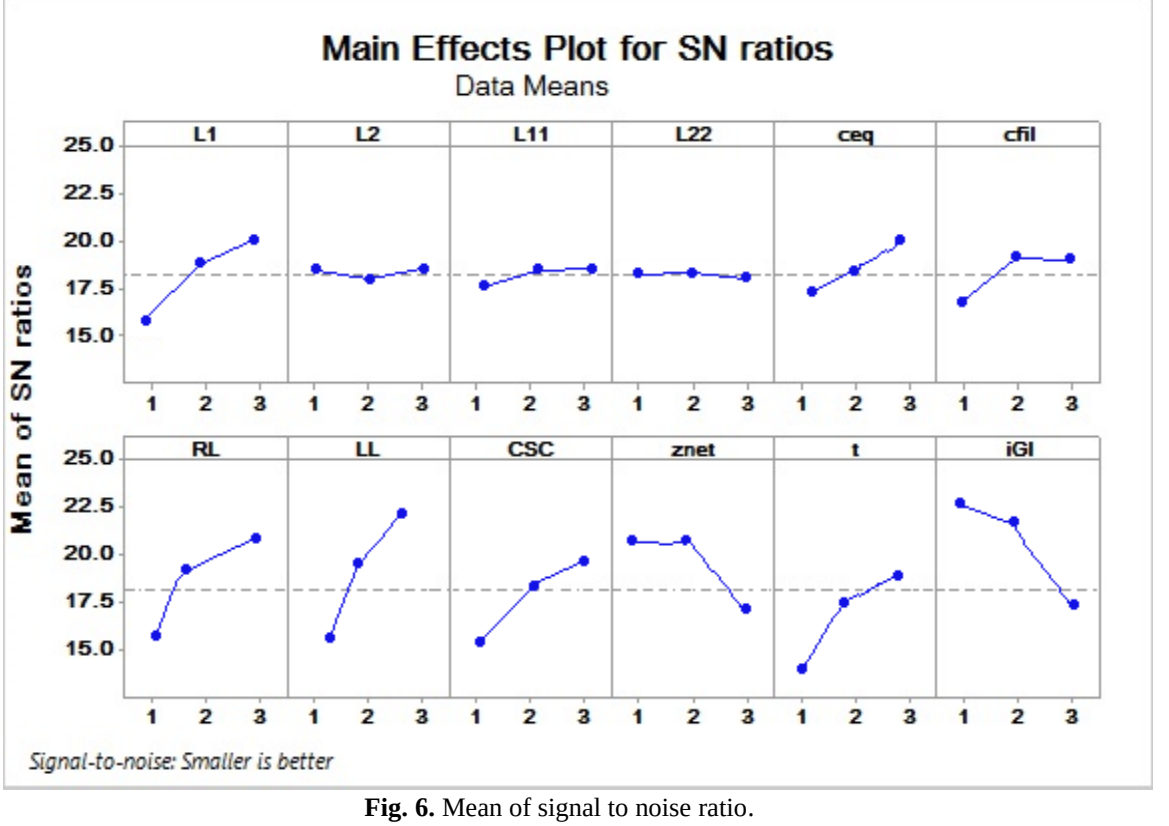

Fig. 6. Mean of signal to noise ratio.

Table 4. Optimal microgrid parameters determined by Taguchi Method.

Parameter	Optimal value	Dimension
L_1	10	mH
L_2	10	mH
R_L	0.5	Ω
L_L	50	mH
Z_{net}	10	Ω
τ	10	S
i_{Gl}	20	A
C_{fil}	0.1	mF
L_{11}	10	mH
C_{eq}	100	mF
L_{22}	0.1	mH
C_{sc}	0.1	F

6. CONCLUSION

This paper presents a new proposed criterion for stability of Phase-Locked loop. Using the new proposed criterion and with the aim of stability improvement of PLL, the optimized rate of microgrid-side and network-side parameters is determined. In this study, the effect of each microgrid-side and network-side parameters on the PLL stability is investigated. To this aim first, the dynamic model of studied microgrid is simulated in MATLAB software and then, a Taguchi approach is employed to determine the optimum levels of the microgrid-side and network side parameters. Moreover, variance analysis is used to prove the meaningful effect of these parameters on the output. Results of statistical analyses show that some microgrid-side and network-side parameters, which have been evaluated in this study, have significant effects on the PLL stability.

REFERENCES

[1] Gh., Anirban, V. John, **" Performance evaluation of three phase SRF-PLL and MAF-SRF-PLL, "** *Turkish Journal of Electrical Engineering & Computer Sciences 23.6*, 2015.

[2] S.Golestan, M. Monfared, F. D. Freijedo, and J. M. Guerrero, **"Design And Tuning Of A Modified Power-Based Pll for Single-Phase Grid-Connected Power Conditioning Systems, "** *IEEE Transactions on Power Electronics*, Vol. 27, 3639-3650, 2012.

[3] K.-J. Lee, J.-P. Lee, D. Shin, D.-W. Yoo, and H.-J. Kim, **"A Novel Grid Synchronization PLL Method Basedon Adaptive Low-Pass Notch Filter for Grid-Connected PCS, "** *IEEE Transactions on Industrial Electronics*, Vol. 61, 292-301, 2014.

[4] S. Golestan, M. Monfared, F. Freijedo, J. M. Guerrero, **"Design And Tuning Of A Modified Power-Based Pll For Single-Phase Grid-Connected Power Conditioning Systems, "** *IEEE Transactions on Power Electronics*, Vol. 27(8), pp. 3639-3650, 2012.

[5] B. Wen, D. Boroyevich, P. Mattavelli, Z. Shen, R. Burgos **"Experimental Verification Of The Generalized Nyquist Stability Criterion For Balanced Three-Phase Ac Systems In The Presence Of Constant Power Loads, "** *In Energy Conversion Congress and Exposition (ECCE)*, IEEE, pp. 3926-3933, 2012.

[6] E. Barklund, N. Pogaku, M. Prodanovic, C. Hernandez-Aramburo, T. C. Green, **"Energy Management In Autonomous Microgrid Using Stability-Constrained Droop Control Of Inverters, "** *IEEE Transactions on Power Electronics*, Vol. 23(5), pp. 2346-2352, 2008.

[7] D. Dong, B. Wen, D. Boroyevich, P. Mattavelli, Y. Xue, **"Analysis Of Phase-Locked Loop Low-Frequency Stability In Three-Phase Grid-Connected Power Converters Considering Impedance Interactions, "** *IEEE Transactions on Industrial Electronics*, Vol. 62(1), pp. 310-321, 2015.

[8] T. L. Hu SH, Lee, C. Y Kuo, J. M. Guerrero**, "A Riding-through Technique for Seamless Transition between Islanded and Grid-Connected Modes of Droop-Controlled Inverters, "** *Energies*, Vol. 9(9), pp. 732, 2016.

[9] J.-r. Kan, N. Li, Z.-l. Yao, Y.-c. Xue, and D.-c. Wu, **" Anti-Islanding Performance Of Grid-Connected Inverters Based On Frequency Droop Pll, "** *7th International Power Electronics and Motion Control Conference (IPEMC)*, pp. 2129-2133, 2012.

[10] D. Dong, , B. Wen, P. Mattavelli, D. Boroyevich, Y. Xue, **" Grid-Synchronization Modeling And Its Stability Analysis For Multi-Paralleled Three-Phase Inverter Systems,** *" In Applied Power Electronics Conference and Exposition (APEC), 2013 Twenty-Eighth Annual IEEE*, pp. 439-446, 2013.

[11] E. Barklund, N. Pogaku, M. Prodanovic, C. Hernandez-Aramburo, and T. C. Green, **" Energy**

Management In Autonomous Microgrid Using Stability-Constrained Droop Control Of Inverters, " *IEEE Transactions on Power Electronics*, Vol. 23, pp. 2346-2352, 2008.

[12] B. Kim, S. Sul, **"Stability-Oriented Design of Frequency Drift Anti-Islanding and Phase-Locked Loop Under Weak Grid, "** *IEEE Journal of Emerging and Selected Topics in Power Electronics*, Vol. 5(2), pp. 760-74, 2017.

[13] E. Barklund, N. Pogaku, M. Prodanovic, C. Hernandez-Aramburo, and T. C. Green, **" Energy Management Inautonomous Microgrid Using Stability-Constrained Droop Control Of Inverters, "** *IEEE Transactions on Power Electronics*, Vol. 23, pp. 2346-2352, 2008.

[14] M. Cespedes, S. Jian, **" Impedance Modeling And Analysis Of Grid-Connected Voltage-Source Converters,"** *IEEE Transactions on Power Electronics 29.3*, pp. 1254-1261, 2014.

[15] F. Gonzalez-Espin, G. Garcerá, I. Patrao, and E. Figueres, **"An Adaptive Control System For Three-Phase Photovoltaic Inverters Working In A Polluted And Variable Frequency Electric Grid,"** *Power Electronics, IEEE Transactions on*, Vol. 27, pp. 4248-4261, 2012.

[16] F. González-Espín, E. Figueres, and G. Garcerá, **" An Adaptive Synchronous-Reference-Frame Phase-Locked Loop For Power Quality Improvement In A Polluted Utility Grid,"** *Ieee Transactions on Industrial Electronics*, Vol. 59, pp. 2718-2731, 2012.

[17] M. Hejri, H. Mokhtari, S. Karimi, and M. R. Azizian, **"Stability Andperformance Analysis Of A Single- Stage Grid-Connectedphotovoltaic System Using Describing Function Theory,"** *International Transactions On Electrical Energy Systems*, Vol. 26, pp. 1898–1916, 2016.

[18] J. R. Kan, N. Li, Z. Yao, Xue, C. Wu, **" Anti-Islanding Performance Of Grid-Connected Inverters Based On Frequency Droop Pll,"** *In Power Electronics and Motion Control Conference (IPEMC), 2012 7th International*, Vol. 3, pp. 2129-2133, 2012.

[19] T. Thacker, R. Burgos, F. Wang, D. Boroyevich, "**Single-Phase Islanding Detection Based On Phase-Locked Loop Stability,"** *In Energy Conversion* Congress and Exposition. 2009. ECCE 2009. IEEE. 3371-3377.

[20] J. Sun, **"Impedance-Based Stability Criterion For Grid-Connected Inverters, "** *IEEE Transactions on PowerElectronics*, Vol. 26, pp. 3075-3078, 2011.